

ROE TYPE SCHEMES FOR THE 2-D
SHALLOW WATER EQUATIONS.

by A. Priestley

Numerical Analysis Report 8/87

The work reported here forms part of the research programme of the Reading/Oxford Institute for Computational Fluid Dynamics and was carried out under SERC Grant no. GR/D/29529.

Introduction

In recent years much effort in the area of computational fluid dynamics, has been spent in approximately solving evolutionary conservation laws where discontinuities in the solution constitute a very important, if not the most important, part of the problem. One of the most successful strategies employed on these problems has been that of the Roe type schemes. These schemes have been designed to provide accurate solutions away from jumps while avoiding the difficulties faced by classical second order accurate schemes, Lax-Wendroff for example, at discontinuities. Other desirable properties such as entropy satisfaction and total variation diminishing (TVD), can be ensured with the scheme.

Why then, apart from sheer esoteric folly, should we want to try applying these schemes to atmospheric and oceanographic flows, governed by the shallow water equations and not normally associated with violent changes? Clearly second order schemes are desirable to achieve accuracy on reasonably sized grids while the shock handling capabilities are retained to cope with the presence of fronts in the atmosphere or tidal surges and bores in the sea for example. Numerous papers, which include Roe et al [8,12], Sells [13], Sweby [14] and Glaister [4,5] have demonstrated the success of Roe type schemes in dealing with discontinuities: here we

concentrate on their ability to compete in the smooth regions.

In Section 1 an introduction to the philosophy behind the Roe approach will be given, and B functions and flux limiters will be introduced as a path towards a variety of methods.

In Section 2 the shallow water equations are stated and the Roe decomposition performed in some detail to obtain the necessary building blocks of the method.

In Section 3 the various methods that can be obtained by this approach are applied to Grammelvedt's problem [7] and it is demonstrated that correct treatment of the source/forcing term is essential. It is shown that schemes capable of handling discontinuities can achieve the same, if not better, accuracy than the more common second order schemes. The experience gained on this problem is then applied to the problem of coastal flow. Here the main source of difficulty is the computationally open boundaries, and their treatment will be discussed.

Finally in Section 4 we will draw some conclusions and make some suggestions about further work that is needed.

1. Roe's Scheme

In this section we give a brief account of the philosophy behind the Roe type schemes, largely following Roe's original paper [8], and refer the reader to that paper for more details.

Consider the initial-value problem for a hyperbolic system of conservation laws

$$\underline{q}_t + \underline{F}_x = 0 \quad (1.1)$$

with initial conditions

$$\underline{q}(x,0) = \underline{q}_0(x), \quad (1.2)$$

where $\underline{F} = \underline{F}(\underline{q})$ and the Jacobian matrix $A = \partial \underline{F} / \partial \underline{q}$ has real eigenvalues.

Introduce now the discrete representation $x_i = x_0 + i\Delta x$, $t_n = t_0 + n\Delta t$ and suppose that \underline{q}_i^n approximates $\underline{q}(x_i, t_n)$. If the initial data (1.2) is specialised to

$$\underline{q}(x,0) = \underline{q}_L \quad (x < 0) \quad ; \quad \underline{q}(x,0) = \underline{q}_R \quad (x > 0) \quad (1.3)$$

then we have a so-called Riemann problem which has been studied copiously and has wavelike solutions. Godunov [6]

produced a numerical scheme for the solution of (1.1) that treats the data as a set of constant states separated by discontinuities at the points $x_{i+\frac{1}{2}}$, say, a Riemann problem then being solved in each interval, with a time-step restriction such that the waves from one jump do not interfere with those from neighbouring jumps.

With the Roe type methods a slightly different approach is taken by considering the approximate problem

$$\underline{q}_t + \tilde{A} \underline{q}_x = 0, \quad (1.4)$$

where $\tilde{A} = \tilde{A}(\underline{q}_L, \underline{q}_R)$ is a constant matrix that is chosen to be representative of the local conditions. A further restriction is that \tilde{A} must satisfy the following properties collectively called Property U:

- (i) It constitutes a linear mapping from the vector space to the vector space \underline{F} .
- (ii) As $\underline{q}_L \rightarrow \underline{q}_R \rightarrow \underline{q}$, $\tilde{A}(\underline{q}_L, \underline{q}_R) \rightarrow A(\underline{q})$ where $A = \partial \underline{F} / \partial \underline{q}$.
- (iii) For any $\underline{q}_L, \underline{q}_R$, $\tilde{A}(\underline{q}_L, \underline{q}_R) \cdot (\underline{q}_L - \underline{q}_R) = \underline{F}_L - \underline{F}_R$.
- (iv) The eigenvectors of \tilde{A} are linearly independent.

Finding an \tilde{A} that satisfies Property U is not a trivial problem. Neither of the two 'obvious' choices $\tilde{A} = \frac{1}{2}(A_L + A_R)$ or $\tilde{A} = A(\frac{1}{2}(\underline{q}_L + \underline{q}_R))$ will in general satisfy (iii), but in the case of (1.4) Roe has shown that one can be found.

This leads to a basic first order upwind scheme for

which at each time-level, at each jump, we calculate the eigenvalues λ_i , the eigenvectors \underline{e}_i , and associated strengths α_i of $\tilde{A}(\underline{q}_L, \underline{q}_R)$. Then the scheme is:

$$\text{if } \left\{ \begin{array}{l} \lambda_i > 0 \\ \lambda_i < 0 \end{array} \right\} \text{ then add } - \frac{\Delta t}{\Delta x} \lambda_i \alpha_i \underline{e}_i \text{ to } \left\{ \begin{array}{l} \underline{q}_R \\ \underline{q}_L \end{array} \right\}. \quad (1.5)$$

[For a two-dimensional problem

$$\underline{q}_t + \underline{F}_x + \underline{G}_y = 0 \quad (1.6)$$

we can calculate $\tilde{A}(\underline{q}_L, \underline{q}_R)$ & $\tilde{B}(\underline{q}_B, \underline{q}_T)$ and solve separately in the x-direction using \tilde{A} and in the y-direction using \tilde{B} . These solutions may then be combined in various ways.]

The basic scheme, (1.5) is only first order and takes discontinuities in its stride, by smoothing them out! It is so diffusive as to be totally inadequate for most problems, and in particular for our applications. The problem then is to find a second order scheme, based on the philosophy previously illustrated, without losing the shock handling properties.

This is achieved by flux limiting, which is essentially done by limiting the anti-diffusive terms in the second order scheme at discontinuities, to avoid the oscillations of classical second order schemes, while retaining second order accuracy in smooth regions of the flow, see Sweby [14,15].

Define $\phi_{j,i+\frac{1}{2}}$ to be the signal from the j^{th} eigenvalue at the jump at $i+\frac{1}{2}$, i.e.

$$\phi_{j,i+\frac{1}{2}} = \frac{-\Delta t}{\Delta x} \lambda_j \alpha_j e_j. \quad (1.7)$$

The algorithm (1.5) then becomes:

$$\text{if } \begin{cases} \lambda_j > 0 \\ \lambda_j < 0 \end{cases} \text{ then add } \phi_{j,i+\frac{1}{2}} \text{ to } \begin{cases} g_{i+1} \\ g_i \end{cases}.$$

If we now transfer an amount $a_{j,i+\frac{1}{2}}$ against the direction of the flow we can achieve second order accuracy in smooth regions by choosing

$a_j = \frac{1}{2}(1-|\nu_j|)$ where ν_j is the CFL number of the j^{th} wave.

Define a transfer function, Baines [1], by

$$B(a_{j,i+\frac{1}{2}} \phi_{j,i+\frac{1}{2}}, a_{j,i+\frac{1}{2}-\sigma_j} \phi_{j,i+\frac{1}{2}-\sigma_j}) = B(b_1, b_2), \quad \text{say,} \quad (1.8)$$

where $\sigma_j = \text{sign}(\lambda_j)$. Choosing $B(b_1, b_2) = b_1$ gives Lax-Wendroff, while $B(b_1, b_2) = \frac{1}{2}(b_1 + b_2)$ corresponds to Fromm's algorithm. (A more comprehensive list of the different B functions that can be used is given in the Appendix.) The two schemes above are classical second order methods and suffer from oscillations at discontinuities. We

can, however, overcome this problem by not restricting ourselves to linear functions of b_1 & b_2 . Sweby [14, 15] introduced a limiter function $\phi(r)$ where $r = b_1/b_2$. The region in $(\phi(r), r)$ space that ensures a TVD (Total Variation Diminishing), i.e. oscillation free scheme, can then be plotted. This region can then be further constrained to ensure oscillation free second order schemes (away from extrema). Sweby [1.4] plotted the minmod, Van Leer and Superbee limiters (see Roe & Baines [11], Van Leer [16], Roe [9]) and showed these to lie in this region. (Two-dimensional algorithms can be constructed that are based on these limiters but also take into account the dimensionality of the problem by including cross terms to eliminate q_{yx} type terms from the truncation error, see Baines [1]). These ideas will now be used in the following sections.

2. Shallow Water Equations

In primitive variables the 2-D shallow water equations relevant to atmospheric flows are given by

$$\phi_t + (\phi u)_x + (\phi v)_y = 0 \quad (2.1a)$$

$$u_t + uu_x + vu_y + \phi_x = \Omega v \quad (2.1b)$$

$$v_t + uv_x + vv_y + \phi_y = -\Omega u, \quad (2.1c)$$

where u & v are the x, y velocities respectively and ϕ is the geopotential ($\phi = gh$ where h is the height of the free surface). Ω is the Coriolis parameter which for the atmospheric flow will be given by the usual β -plane approximation and for the coastal flow problem will be taken to be a constant.

To apply Roe's scheme to these equations we need to rewrite them in conservative form. Replacing x & y velocities by x & y momenta ($m = u\phi$, $n = v\phi$) we get

$$\phi_t + m_x + n_y = 0 \quad (2.2a)$$

$$m_t + \left[\frac{m^2}{\phi} + \frac{\phi^2}{2} \right]_x + \left[\frac{mn}{\phi} \right]_y = \Omega n \quad (2.2b)$$

$$n_t + \left[\frac{mn}{\phi} \right]_x + \left[\frac{n^2}{\phi} + \frac{\phi^2}{2} \right]_y = -\Omega m. \quad (2.2c)$$

This can now be written in a vector flux form as

$$\underline{q}_t + \underline{F}_x + \underline{G}_y = \underline{b}$$

where

$$\underline{q} = \begin{bmatrix} \phi \\ m \\ n \end{bmatrix}, \quad \underline{F} = \begin{bmatrix} m \\ \frac{m^2}{\phi} + \frac{\phi^2}{2} \\ \frac{mn}{\phi} \end{bmatrix}, \quad \underline{G} = \begin{bmatrix} n \\ \frac{m n}{\phi} \\ \frac{n^2}{\phi} + \frac{\phi^2}{2} \end{bmatrix}$$

$$\text{and } \underline{b} = \begin{bmatrix} 0 \\ \Omega n \\ -\Omega m \end{bmatrix}.$$

Following Roe [8] we define an intermediate, or parameter, vector

$$\underline{w} = \begin{bmatrix} w_1 \\ w_2 \\ w_3 \end{bmatrix} = \begin{bmatrix} \phi^{\frac{1}{2}} \\ \phi^{\frac{1}{2}} u \\ \phi^{\frac{1}{2}} v \end{bmatrix}$$

and now express the vectors \underline{q} , \underline{F} & \underline{G} in terms of the intermediate vector to get

$$\underline{q} = \begin{bmatrix} w_1^2 \\ w_1 w_2 \\ w_1 w_3 \end{bmatrix}, \quad \underline{F} = \begin{bmatrix} w_1 w_2 \\ w_2^2 + \frac{w_1}{2} \\ w_2 w_3 \end{bmatrix}, \quad \underline{G} = \begin{bmatrix} w_1 w_3 \\ w_2 w_3 \\ w_3^2 + \frac{w_1}{2} \end{bmatrix}.$$

Using the standard notation of $\Delta \underline{x} = \underline{x}_R - \underline{x}_L$ and $\bar{\underline{x}} = \frac{1}{2}(\underline{x}_R + \underline{x}_L)$ we proceed to calculate matrices $B(\underline{w})$ & $C(\underline{w})$ such that

$$\Delta \underline{q} = B(\underline{w}) \Delta \underline{w}$$

$$\Delta \underline{F} = C(\underline{w}) \Delta \underline{w}.$$

This leads to

$$B = \begin{bmatrix} 2\bar{w}_1 & 0 & 0 \\ \bar{w}_2 & \bar{w}_1 & 0 \\ \bar{w}_3 & 0 & \bar{w}_1 \end{bmatrix},$$

$$C = \begin{bmatrix} \bar{w}_2 & \bar{w}_1 & 0 \\ 2\bar{w}_1 \bar{w}_1^2 & 2\bar{w}_2 & 0 \\ 0 & \bar{w}_3 & \bar{w}_2 \end{bmatrix}.$$

We now find λ such that

$$\det (\lambda B - C) = 0,$$

giving

$$\lambda_{1,2,3}^F = \frac{\bar{w}_2}{\bar{w}_1} - \sqrt{\frac{\bar{w}_2^2}{\bar{w}_1^2}}, \frac{\bar{w}_2}{\bar{w}_1}, \frac{\bar{w}_2}{\bar{w}_1} + \sqrt{\frac{\bar{w}_2^2}{\bar{w}_1^2}}$$

which are seen to be the $u, u \pm \sqrt{\phi}$ characteristic speeds we would have expected.

These eigenvalues give three eigenvectors which, after multiplication by B, are given by: -

$$\underline{e}_{1,2,3}^F = \left\{ \begin{array}{c} \bar{w}_1 \\ w_2 - w_1 \sqrt{\frac{\bar{w}_2^2}{\bar{w}_1^2}} \\ \bar{w}_3 \end{array} \right\}, \left\{ \begin{array}{c} 0 \\ 0 \\ \bar{w}_1 \end{array} \right\}, \left\{ \begin{array}{c} \bar{w}_1 \\ \bar{w}_2 + \bar{w}_1 \sqrt{\frac{\bar{w}_2^2}{\bar{w}_1^2}} \\ \bar{w}_3 \end{array} \right\}.$$

It is noted here for future reference that, if regarded as a 3x3 matrix, the inverse of the above is given by:-

$$\frac{1}{2\bar{w}_1^2 \sqrt{\frac{\bar{w}_2^2}{\bar{w}_1^2}}} \begin{pmatrix} \bar{w}_2 + \bar{w}_1 \sqrt{\frac{\bar{w}_2^2}{\bar{w}_1^2}} & -\bar{w}_1 & 0 \\ -2\bar{w}_3 \sqrt{\frac{\bar{w}_2^2}{\bar{w}_1^2}} & 0 & 2\bar{w}_1 \sqrt{\frac{\bar{w}_2^2}{\bar{w}_1^2}} \\ -(\bar{w}_2 - \bar{w}_1 \sqrt{\frac{\bar{w}_2^2}{\bar{w}_1^2}}) & \bar{w}_1 & 0 \end{pmatrix}. \quad (2.3)$$

Three α 's are now found such that

$$\sum_i \alpha_i \underline{e}_i = \Delta \underline{q} \quad (\text{and by construction } \sum_i \alpha_i \lambda_i \underline{e}_i = \Delta \underline{F}), \text{ i.e.}$$

$$\begin{Bmatrix} \alpha_1^F \\ \alpha_2^F \\ \alpha_3^F \end{Bmatrix} = \begin{Bmatrix} \Delta w_1 - \frac{\bar{w}_1 \Delta w_2 - \bar{w}_2 \Delta w_1}{2\bar{w}_1 \sqrt{\bar{w}_1^2}} \\ \frac{\bar{w}_1 \Delta w_3 - \bar{w}_3 \Delta w_1}{\bar{w}_1} \\ \Delta w_1 + \frac{\bar{w}_1 \Delta w_2 - \bar{w}_2 \Delta w_1}{2\bar{w}_1 \sqrt{\bar{w}_1^2}} \end{Bmatrix}.$$

Performing similar operations in the y-direction gives

$$\lambda_{1,2,3}^G = \frac{\bar{w}_3}{\bar{w}_1} - \sqrt{\bar{w}_1^2}, \quad \frac{\bar{w}_3}{\bar{w}_1}, \quad \frac{\bar{w}_3}{\bar{w}_1} + \sqrt{\bar{w}_1^2} \quad \text{with}$$

$$\underline{e}_{1,2,3}^G = \left\{ \begin{array}{l} \begin{bmatrix} \bar{w}_1 \\ \bar{w}_2 \\ \bar{w}_3 - \bar{w}_1 \sqrt{\bar{w}_1^2} \end{bmatrix} \begin{bmatrix} 0 \\ \bar{w}_1 \\ 0 \end{bmatrix} \begin{bmatrix} \bar{w}_1 \\ \bar{w}_2 \\ \bar{w}_3 + \bar{w}_1 \sqrt{\bar{w}_1^2} \end{bmatrix} \end{array} \right\}$$

and

$$\begin{Bmatrix} \alpha_1^G \\ \alpha_2^G \\ \alpha_3^G \end{Bmatrix} = \begin{Bmatrix} \Delta w_1 - \frac{\bar{w}_1 \Delta w_3 - \bar{w}_3 \Delta w_1}{2\bar{w}_1 \sqrt{\bar{w}_1^2}} \\ \frac{\bar{w}_1 \Delta w_2 - \bar{w}_2 \Delta w_1}{\bar{w}_1} \\ \Delta w_1 + \frac{\bar{w}_1 \Delta w_3 - \bar{w}_3 \Delta w_1}{2\bar{w}_1 \sqrt{\bar{w}_1^2}} \end{Bmatrix}.$$

These eigenvalues, eigenvectors and wave strengths are used to decompose the problem into wave type components to which algorithm (1.5) can then be applied.

3. Model Problems

In this section two model problems will be discussed that will force us to consider different aspects of the method to ensure a worthwhile solution.

(i) The first is an atmospheric flow using the equations in the form given in (2.2). It is known as Grammelvedt's problem with initial conditions 1 (see Grammelvedt [7]) and concerns a flat bottomed channel 6000 km x 4400 km. The north/south boundaries are taken to be rigid walls, making the Great Wall of China look small, and the flow is assumed periodic in the east/west direction. The initial conditions for the height and velocity field are shown in Figures 1 & 2.

This problem is particularly useful because, aside from calculating the actual solution, it is quite straightforward in that the geometry is rectangular and the boundary conditions are easy to write down. Due to the nature of the problem the available energy, given by

$$AE = \frac{1}{2g} \int_{\sigma} \{ (u^2 + v^2 - \phi) - \bar{\phi}^2 \} d\phi, \quad (3.1)$$

where $\bar{\phi}$ is the average value of the geopotential of the free surface and σ is the domain, is conserved. Hence, by monitoring this quantity, we can measure the success of our efforts without knowing the exact solution to the problem. It is worth just noting here that conserving 100% of the

available energy is necessary for an exact solution but it is not a sufficient condition.

A numerical scheme is deemed to have become unstable when the available energy has risen by 10%. With some of the results the comments "going unstable" or "about to go unstable" have been added, which indicates that although we have not reached the 10% criterion the available energy for that particular method had started to increase, to a greater or lesser extent, and would, by our definition, have become unstable very rapidly thereafter.

We use a 200 km grid (30 x 22) and take time-steps of 5 minutes. The results in Table 1 correspond to the percentage of the available energy left after 5 days.

First Order	:-	3.9%	
Lax-Wendroff	:-	60 %	(going unstable)
2nd order fully upwinded	:-	42 %	
Fromm's algorithm	:-	43.5%	
3rd order split	:-	45 %	
Minmod	:-	23 %	
Superbee	:-	66.3%	(going unstable)
Minmod (2-D)	:-	32.3%	

Table 1

As can be seen these results do lack a certain something, namely rather a lot of energy. The schemes that come out best are the more classical second order methods, although as with all these schemes the time-step must be

restricted because the CFL numbers are given by $u\Delta t/\Delta x$ & $(u+\sqrt{\phi})\Delta t/\Delta x$, and the $u+\sqrt{\phi}$ values are an order of magnitude larger than the u characteristic. The methods, though, are explicit finite differences and so this time-step restriction is not too much of a problem. Reducing the time-step to stabilize the Lax-Wendroff and Superbee methods still only leaves us with just over 50%. Using the 'genuinely two-dimensional' minmod scheme does, in this case, do better than its 1-D version, although there are also examples where it does fractionally worse, but it still is a long way behind the other methods and is computationally very much more expensive to calculate.

However, all is not yet lost. So far the right hand side of the shallow water equations, $\underline{b} = (0, \Omega n, -\Omega m)^T$, has been studiously ignored. For the shallow water equations, in this context, the Coriolis force is a significant term of equal magnitude to the $(\phi^2/2)_x$ & $(\phi^2/2)_y$ terms, the geostrophic approximation. The results in Table 1 were all obtained by evaluating the Coriolis force pointwise and using this value to update at that particular gridpoint. In the light of the previous sentence we should perhaps not be treating these terms so flippantly.

Roe [10] shows how to deal with source terms by considering the simplest problem of any relevance to us, the scalar wave equation

$$u_t + au_x = b(x) \quad (3.2)$$

where a is a positive constant. The initial-value problem

for (3.2) with initial data $u = u_0(x)$ has the general solution

$$u(x,t) = u_0(x-at) + \frac{1}{a} \int_{x-at}^x b(x) dx \quad (3.3)$$

In practice the integrand in (3.3) will depend on the solution u , for which we only have information at the previous time-level, and hence we would expect to approximate the integral by

$$\frac{1}{a}(x-(x-at)) b(x-at) = tb(x-at).$$

Hence the source term ought to be upwinded in the same way as the other term.

Glaister [5] has considered the 2-D Euler equations in r, z variables with cylindrical geometry. (Here the 'source' terms are due to the expansion of the grid in the radial direction.) These source terms were expanded in the eigenvectors associated with the radial direction and upwinded according to the corresponding eigenvalue. This procedure was found to significantly improve the results.

Our problem is slightly different in that in vector form

$$\underline{q}_t + \underline{F}_x + \underline{G}_y = \underline{b}$$

We have one right hand side vector but two sets of eigenvectors in which to expand it, with no immediately clear way of splitting \underline{b} into $\underline{b}^A + \underline{b}^B$ prior to expansion in

terms of the eigenvectors of A or B. One of the options is to take

$$\underline{b}^A = \begin{bmatrix} 0 \\ \Omega n \\ 0 \end{bmatrix} \quad \& \quad \underline{b}^B = \begin{bmatrix} 0 \\ 0 \\ -\Omega m \end{bmatrix}, \quad (3.4)$$

that is expand the source term associated with the x-momentum equation in the x-orientated eigenvectors and similarly for y. This sounds eminently reasonable but it is not at all clear from the vector equation why this should be done, and what treatment should be given to a source term in the ϕ equation which has no associated direction. Another option is to take

$$\underline{b}^A = \underline{b}^B = \frac{1}{2}\underline{b}. \quad (3.5)$$

In order to expand the forcing terms in the eigenvectors we need to know weights for each eigenvector. In the x-direction this is done by multiplying the vector to be projected, \underline{b}^A , by the matrix (2.3), a similar operation being done to \underline{b}^B . This gives the weights associated with $\underline{e}_{1,2,3}^F$ & $\underline{e}_{1,2,3}^G$ as

$$\frac{\Omega \bar{w}_3}{2\sqrt{\bar{w}_1^2}} (1, 0, -1) \quad \& \quad \frac{-\Omega \bar{w}_2}{2\sqrt{\bar{w}_1^2}} (1, 0, -1) \quad (3.6)$$

for the first option, (3.4), and

$$\frac{\Omega}{4\sqrt{\bar{w}_1^2}} (\bar{w}_3, 2\bar{w}_2\sqrt{\bar{w}_1^2}, -\bar{w}_3) \quad \& \quad \frac{-\Omega}{4\sqrt{\bar{w}_1^2}} (\bar{w}_2, 2\bar{w}_3\sqrt{\bar{w}_1^2}, -\bar{w}_2) \quad (3.7)$$

for the second option (3.5).

For the first case we choose to average Ωn by $\Omega \bar{w}_1 \bar{w}_3$, because it marginally simplifies the expressions in (3.6). However, the schemes do not seem very sensitive to the averaging used in the evaluation of \underline{b} , $\Omega w_1 w_3$ giving the same results. Both these options give marked increases in accuracy but it is the first that gives the best, and the results for this strategy are given below in Table 2 for some of the schemes, using 4 minute time-stepping.

First Order	:-	72.4%
L-W	:-	85.9% (about to go unstable)
2nd order	:-	87 % (about to go unstable)
Fromm	:-	85 %
3rd order	:-	85.4%
Minmod	:-	77.3%
Superbee	:-	86.9% (about to go unstable)
Minmod (2-D)	:-	78 %
Fromm limiter	:-	82 %
Van Leer	:-	80 %

Table 2

The effect of cross-terms becomes less significant as the time-step is reduced because they are $O(\Delta t^2)$.

Reducing the time-step to stabilize Superbee we obtain the following results

3 min	:-	87.8%
2 min	:-	90.4%
90 sec	:-	92.8%

2-D Superbee with the 3 min. time-stepping gives 88%, reinforcing the claim about the cross terms. These results are actually better than the classical methods give us with reduced time-stepping, but the Superbee scheme can still cope with discontinuities. These results are a considerable improvement over our previous table, showing the importance of correctly dealing with source/forcing terms. Figures 3,4,5 show the height, velocity field and available energy for the Van Leer limiter, figures 6,7,8 show the same sequence for Fromm's scheme while figures 9,10,11 show the results for Superbee with 2 minute time-stepping.

(ii) The second model problem is that of coastal flow. The equations used here are

$$u_t + uu_x + vu_y + gz_x + \frac{Fu\sqrt{u^2 + v^2}}{h + z} - \Omega v = 0 \quad (3.8a)$$

$$v_t + uv_x + vv_y + gz_y + \frac{Fv\sqrt{u^2 + v^2}}{h + z} + \Omega u = 0 \quad (3.8b)$$

$$z_t + (u(h + z))_x + (v(h + z))_y = 0, \quad (3.8c)$$

where h is the depth of the sea bed, below some fixed level and z is the elevation above this level i.e. total depth is

$h + z$. The new term is a friction term and F is the friction factor ($0(10^{-3})$). Our conserved variables are then $g(h + z)$, $g(h + z)u$, $g(h + z)v$, much as before. The only real differences from before are the addition of a potentially variable seabed and the addition of the friction terms to the right hand side. The Roe decomposition goes through as previously. The energy is no longer conserved, due to the presence of friction, and so these equations possess no easy guide to the success of the approximation. We will therefore use our experience with Grammelvedt's problem to choose the appropriate methods.

The real problem posed by this model problem is the treatment of the boundary conditions. We shall take as our problem a straight stretch of coastline 50 kms long. This presents no problems as it is treated as a rigid wall as in Grammelvedt's problem. Even if the various Governments of the countries around the North Sea (particularly the Norwegians who would have an extremely difficult task) could be persuaded to straighten out their respective coastlines to make a rectilinear domain of the North Sea we are still left with the problem that we are only really interested in the flow close to the shore and do not want the expense of calculating the entire flow.

As our model problem, then, we take a (10 x 50) km region with the rigid wall to the west and the southern, eastern and northerly boundaries open. Assuming that the flow is sub-critical we shall need one boundary condition on outflow and two on inflow boundaries for the exact problem.

Edwards, Please and Preston [3] have discussed stable boundary conditions for the linearised shallow water equations. A problem with many finite difference techniques is that they require more boundary conditions than the mathematical problem and this can cause severe problems (see Burgess [2]). Using a scheme based on characteristics, though, means that we only need to use the correct number of boundary conditions, and those suggested by Edwards et al will be used. These are (i) elevation prescribed at outflow and (ii) elevation and tangential velocity given at inflow.

The initial conditions are taken from an exact solution to the 2-D wave equation, namely

$$u = 0 \quad (3.9a)$$

$$v = \frac{Ag}{\sqrt{gh}} \sin \left[\frac{2\pi}{P} \left(\frac{y}{\sqrt{gh}} - t \right) \right] \quad (3.9b)$$

$$z = A \sin \left[\frac{2\pi}{P} \left(\frac{y}{\sqrt{gh}} - t \right) \right] \quad (3.9c)$$

where $A = 1.0$ m is the tidal amplitude and $P = 12.42$ hrs is the tidal period. The initial values are plotted in Figure 12. Formulae 3.9 are not only used to give the initial conditions but are also used to prescribe the boundary conditions as well. Unfortunately the solution described by equations 3.9 rapidly lost touch with reality at the seaward boundary and so the region was extended to $0 < x < 20$, $-25 < y < 75$ km and the boundary conditions applied on these boundaries to try to minimize their effect on the region of interest.

Figure 13 shows the solution generated by using the first order method with 30 second time-stepping and Figure 14 shows the solution given by Superbee with 10 second time-stepping, plotted after six hours. These show quite similar results and demonstrate the stability of the Superbee algorithm in this situation.

4. Conclusion

It is well known that the Roe type flux limited schemes provide a very powerful tool for resolving flows where discontinuities form a major part. In this paper smooth flows with forcing terms have been concentrated upon and the methods have been shown to be, if anything, even more accurate than the more classical second order schemes. The ease of applying boundary conditions is another advantage over non-characteristic based schemes. This would imply that the methods may be useful for flows where discontinuities are only a possibility rather than the be-all and end-all of the calculation.

Further work now being done is to reformulate Roe's scheme to apply to non-rectangular domains, a very necessary step for physical 2-D calculations, and to produce a method that is not as limited in CFL number so as to offset the extra expense of the decomposition.

5. Acknowledgements

The author wishes to thank Dr. M.J. Baines for supervising this work and to P. Glaister for many useful discussions. The financial support of the SERC is gratefully acknowledged.

6. References

- [1] Baines, M.J., "Numerical Algorithms for the Non-linear Scalar Wave Equation". University of Reading, Numerical Analysis Report 1/83 (1983).
- [2] Burgess, N.A., "The Stability of an Approximation to the 1-D Shallow Water Equations" O.U.C.L. Report Number 86/8 (1986).
- [3] Edwards, N.A., Please, C.P., Preston, R.W., "Some Observations on Boundary Conditions for the Shallow-water Equations in Two Space Dimensions", IMA Journal of Applied Mathematics, 30 (1983).
- [4] Glaister, P., "Flux Difference Splitting Techniques for the Euler Equations in Non-Cartesian Geometry", University of Reading. Numerical Analysis Report 8/85 (1985).
- [5] Glaister, P., "Second Order Difference Schemes for Hyperbolic Conservation Laws with Source Terms", University of Reading. Numerical Analysis Report 6/87 (1987).
- [6] Godunov, S.K., "A Finite Difference Method for the Numerical Computation of Discontinuous Solutions of the Equations of Gas Dynamics, Mat Sb. 47 (1959).
- [7] Grammelvedt, A., "A Survey of Finite-Difference Schemes for the primitive equations for a Barotropic Fluid", Monthly Weather Review Vol. 97, No. 5 (1969).
- [8] Roe, P.L., "Approximate Riemann Solvers, Parameter Vectors, and Difference Schemes", Journal of Computational Physics, 43 (1981).
- [9] Roe, P.L., "Some Contributions to the Modelling of Discontinuous Flows, "Lectures in Applied Mathematics, 22, part 2. Am. Math. Soc. (1985).
- [10] Roe, P.L., "Upwind Differencing Schemes for Hyperbolic Conservation Laws with Source Terms", Proc. 1st Int. Congress on Hyperbolic Problems, St. Etienne (1986).
- [11] Roe, P.L. and Baines, M.J., "Algorithms for Advection and Shock Problems", Proc. 4th GAMM Conf. on Numerical Methods in Fluid Mechanics, (Ed. H. Viviand), Vieweg (1982).

- [12] Roe, P.L. and Pike, J., "Efficient Construction and Utilisation of Approximate Riemann Solutions", Computing Methods in Applied Science and Engineering, VI, 499 (1984).
- [13] Sells, C.C.L., "Solution of the Euler Equations for Transonic Flow Past a Lifting Aerofoil", R.A.E. Technical Report 80065 (1980).
- [14] Sweby, P.K., "High Resolution Schemes using Flux Limiters for Hyperbolic Conservation Laws", SIAM Journal of Numerical Analysis, Vol. 21, No. 5 (1984).
- [15] Sweby, P.K., "High Resolution TVD Schemes Using Flux Limiters", Lectures in Applied Mathematics, Vol. 22 (1985).
- [16] Van Leer, B., "Towards the Ultimate Conservative Difference Scheme II. Monotonicity and Conservation combined in a Second Order Scheme". J. Computational Physics, 32 (1974).

Appendix B function

First Order	$B(b_1, b_2) = 0$
Lax-Wendroff	$B(b_1, b_2) = b_1$
Second Order Fully upwinded	$B(b_1, b_2) = b_2$
Fromm's algorithm	$B(b_1, b_2) = \frac{1}{2}(b_1 + b_2)$
Third Order	$B(b_1, b_2) = \frac{1}{3}((2-\nu)b_1 + (1+\nu)b_2)$ (ν is the CFL no.)
Minmod	$B(b_1, b_2) = \begin{cases} b_1 & \text{if } b_1 < b_2 \\ b_2 & \text{if } b_1 > b_2 \end{cases}$
Fromm based limiter	$B(b_1, b_2) = \begin{cases} \frac{1}{2}(b_1 + b_2) & \frac{1}{3} < \frac{b_1}{b_2} < 3 \\ 2 \text{ minmod}(b_1, b_2) & \text{otherwise} \end{cases}$ if $b_1 b_2 > 0$ and zero otherwise
Van Leer limiter	$B(b_1, b_2) = \begin{cases} \frac{2b_1 b_2}{(b_1 + b_2)} & b_1 b_2 > 0 \\ 0 & \text{otherwise} \end{cases}$
Superbee	$B(b_1, b_2) = \begin{cases} b_1 & 1 \leq \frac{b_1}{b_2} \leq 2 \\ b_2 & 1 \leq \frac{b_2}{b_1} \leq 2 \\ 2b_2 & \frac{b_1}{b_2} \geq 2 \\ 2b_1 & \frac{b_2}{b_1} \geq 2 \end{cases}$ if $b_1 b_2 > 0$ 0 otherwise

Hyperbee

$$B(b_1, b_2) = \begin{cases} b_1 & 1 \leq \frac{b_1}{b_2} \leq 2 + \frac{2\nu}{1-\nu} \\ b_2 & 1 \leq \frac{b_2}{b_1} \leq 2 + \frac{2(1-\nu)}{\nu} \\ 2 + \frac{2\nu}{1-\nu} b_2 & \frac{b_1}{b_2} \geq 2 + \frac{2\nu}{1-\nu} \\ 2 + \frac{2(1-\nu)}{\nu} b_1 & \frac{b_2}{b_1} \geq 2 + \frac{2(1-\nu)}{\nu} \end{cases}$$

if $b_1 b_2 > 0$

0 otherwise.

Ultrabee

$$\phi(r) = \frac{2r}{\nu(1-\nu)} \frac{\nu(1-r) + r(1-r^{-\nu})}{(1-r^2)}$$
$$B(b_1, b_2) = b_2 \phi(r) \text{ if } b_1 b_2 > 0$$

0 otherwise.

14.10.1987
k.h.b.

GRAMMELTVEDT'S PROBLEM

Solution, calculated by the Superbee scheme using
0 time-steps with $\Delta t = 0.00$ and $\Delta x = 200$ km.,
Initial conditions 1 were used.

The maximum height is 2214.1 metres at $\#$ and the minimum height is 1785.9 metres at $\#$.

Contour Key

1	→	1800.0
2	→	1850.0
3	→	1900.0
4	→	1950.0
5	→	2000.0
6	→	2050.0
7	→	2100.0
8	→	2150.0
9	→	2200.0

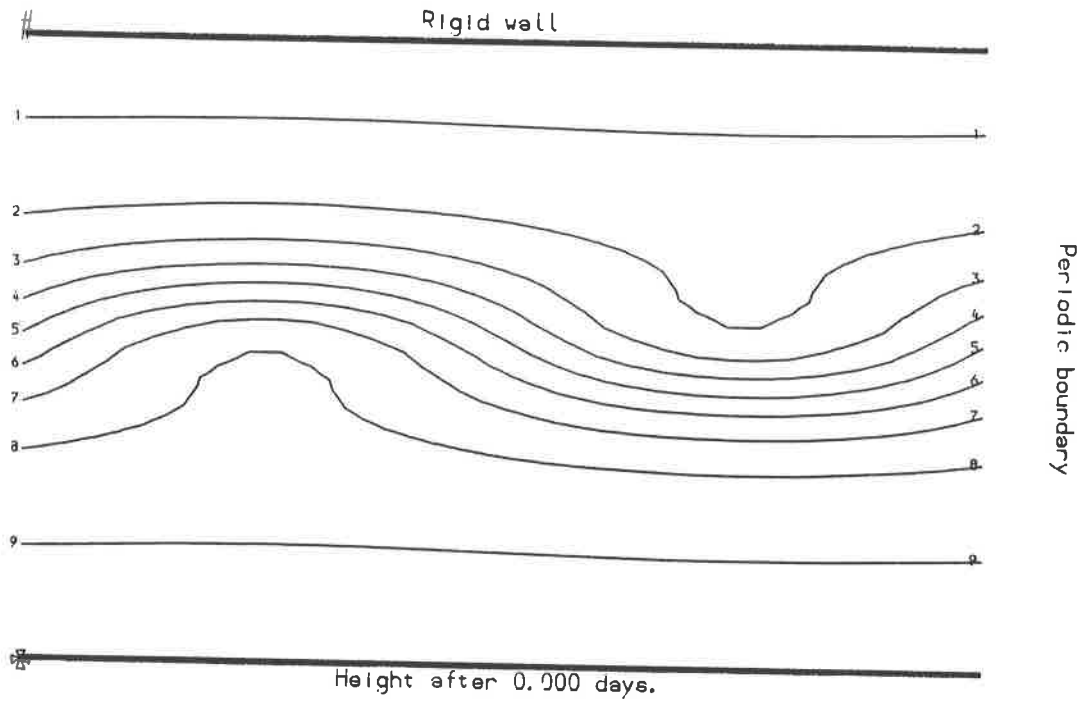


Figure 1

GRAMMELTVEDT'S PROBLEM

Solution, calculated by the Superbee scheme using

0 time-steps with $\Delta t = 0.00$ and $\Delta x = 200$ km.

Initial conditions 1 were used.

The maximum wind speed is 43.206 metres per second.

(96.65 m.p.h.)

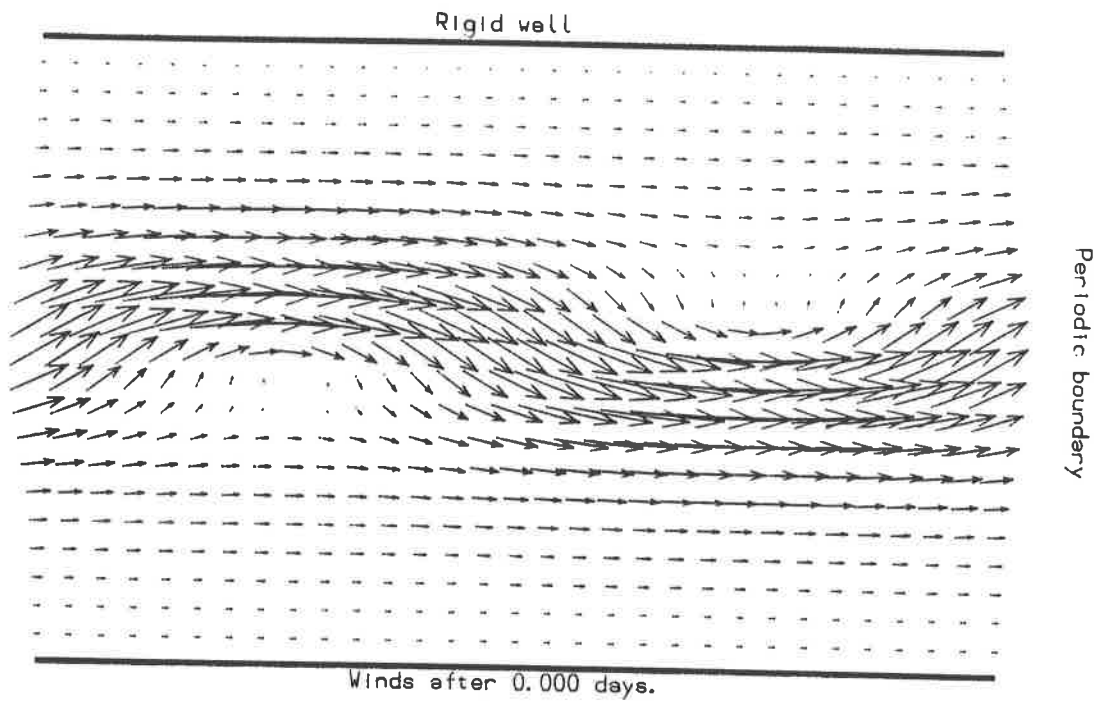


Figure 2

GRAMMELTVEDT'S PROBLEM

Solution, calculated by a Van-Leer limited scheme using
1800 time-steps with $\Delta t = 240.00$ and $\Delta x = 200$ km.

Initial conditions 1 were used.

The transfer function, $B(b_1, b_2)$, is given by $B = 2.0 * b_1 * b_2 / (b_1 + b_2)$.

The maximum height is 2214.7 metres at $\frac{1}{2}$ and the minimum height is 1784.5 metres at $\frac{1}{2}$.

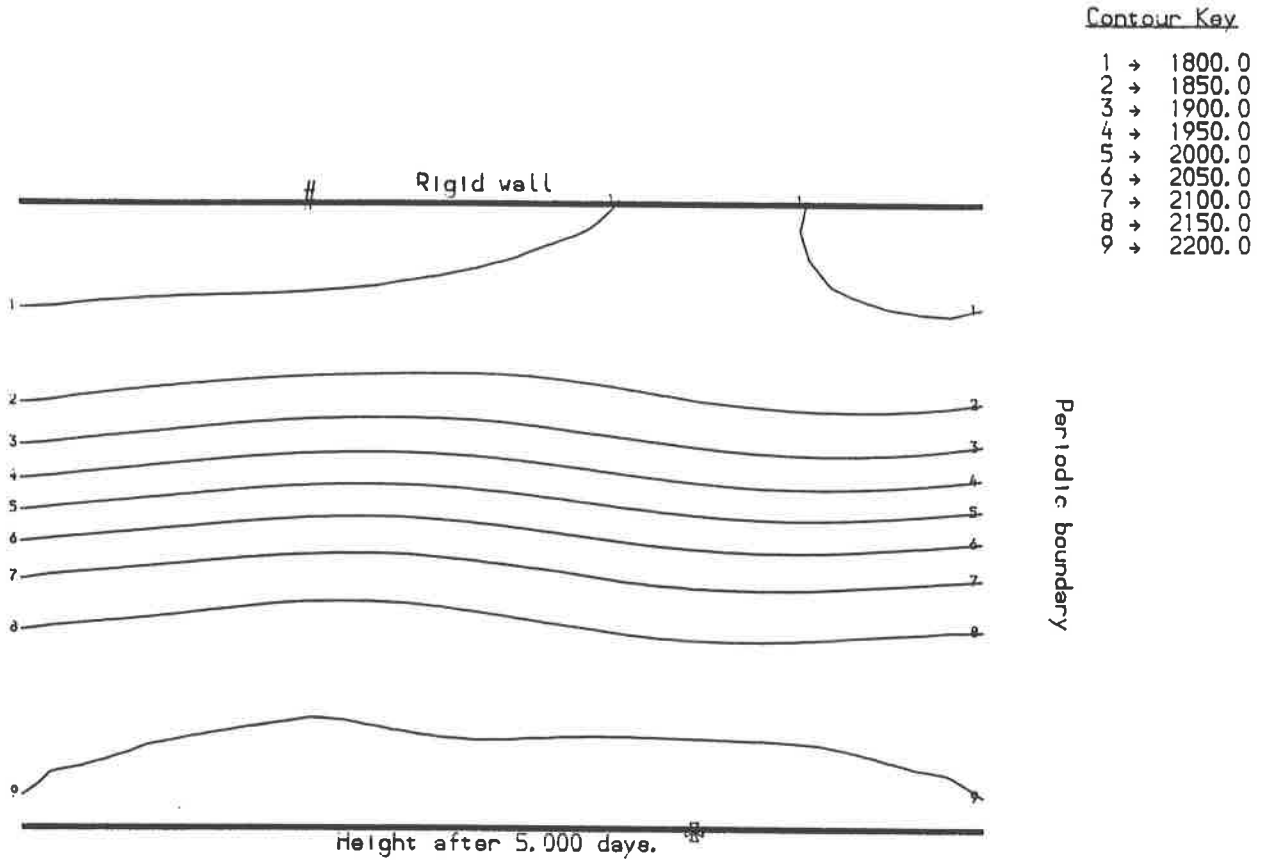


Figure 3

GRAMMELTVEDT'S PROBLEM

Solution, calculated by a Van-Leer limited scheme using
1800 time-steps with $\Delta t = 240.00$ and $\Delta x = 200$ km..

Initial conditions 1 were used.

The transfer function, $B(b_1, b_2)$, is given by $B = 2.0 * b_1 * b_2 / (b_1 + b_2)$.

The maximum wind speed is 23.301 metres per second.

(52.12 m.p.h..)

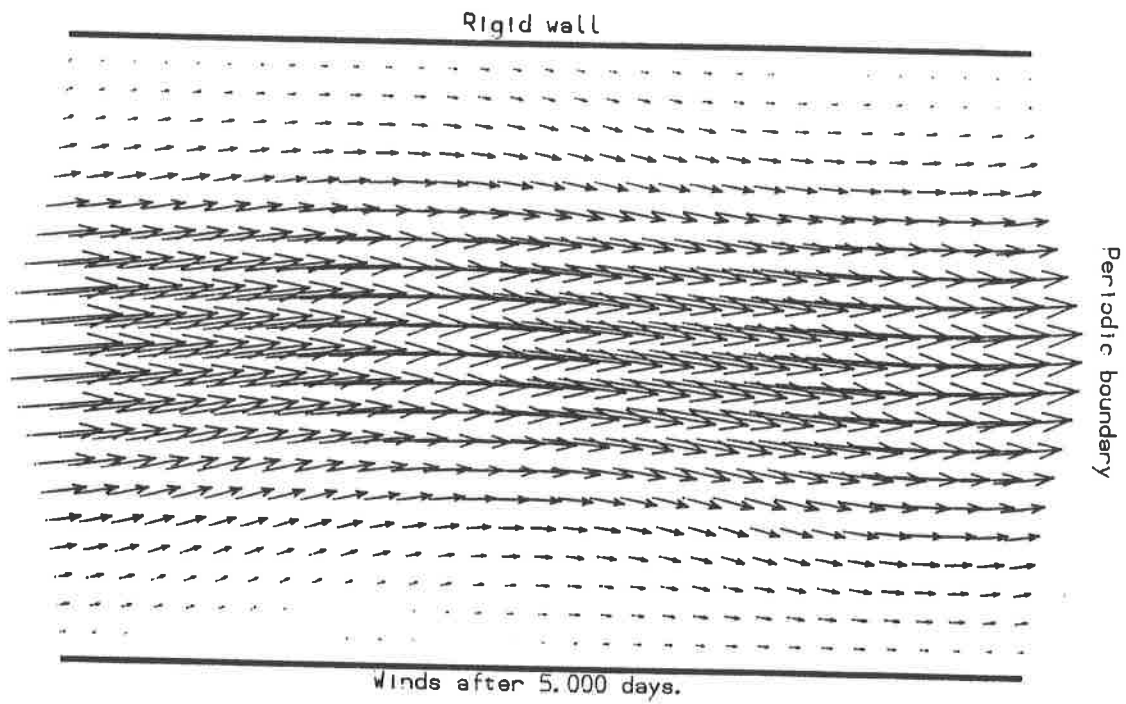


Figure 4

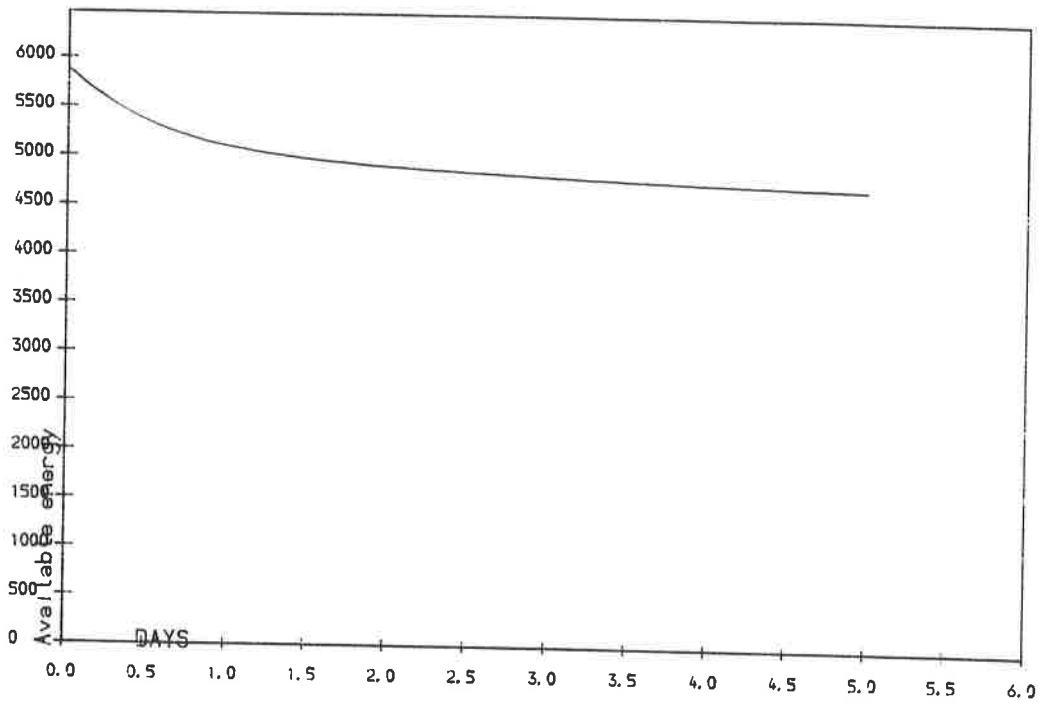


Figure 5

GRAMMELTVEDT'S PROBLEM

Solution, calculated by the split Fromm algorithm using
1800 time-steps with $\Delta t = 240.00$ and $\Delta x = 200$ km.

Initial conditions 1 were used.

The transfer function, $B(b_1, b_2)$, is given by $B = 0.5 * (b_1 + b_2)$

The maximum height is 2234.6 metres at x_0 and the minimum height is 1765.2 metres at x_1 .

Contour Key

1	→	1800.0
2	→	1850.0
3	→	1900.0
4	→	1950.0
5	→	2000.0
6	→	2050.0
7	→	2100.0
8	→	2150.0
9	→	2200.0

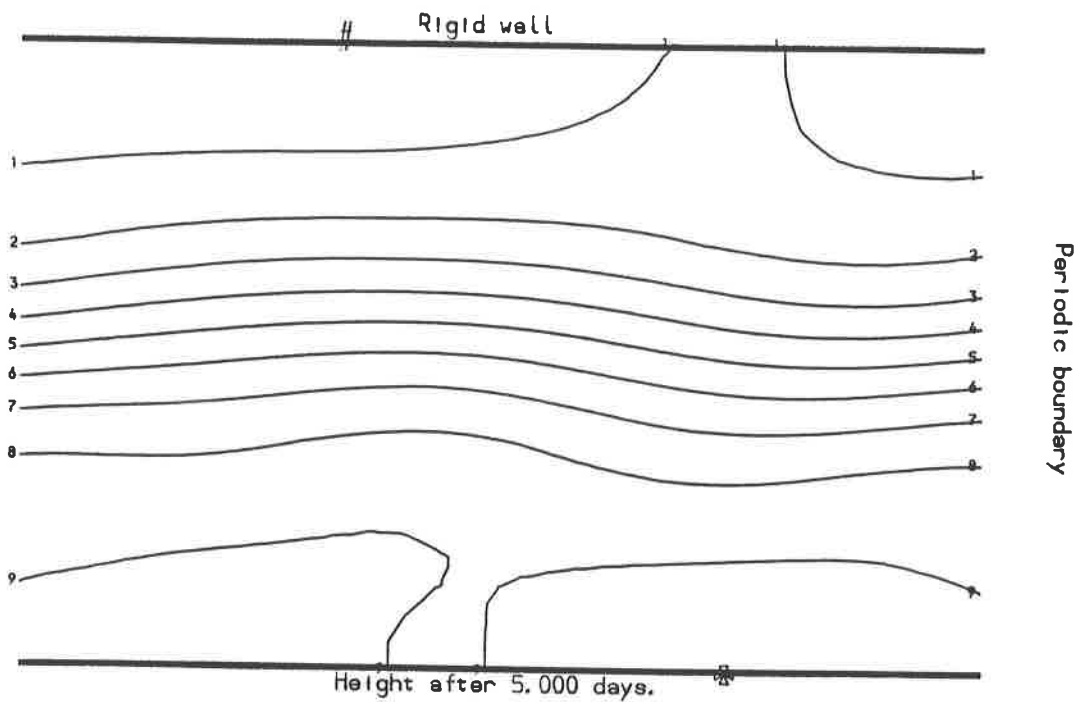


Figure 6

GRAMMELTVEDT'S PROBLEM

Solution, calculated by the split Fromm algorithm using
1800 time-steps with $\Delta t = 240.00$ and $\Delta x = 200$ km.

Initial conditions 1 were used.

The transfer function, $B(b_1, b_2)$, is given by $B = 0.5 * (b_1 + b_2)$

The maximum wind speed is 24.293 metres per second.
(54.34 m. p. h.)

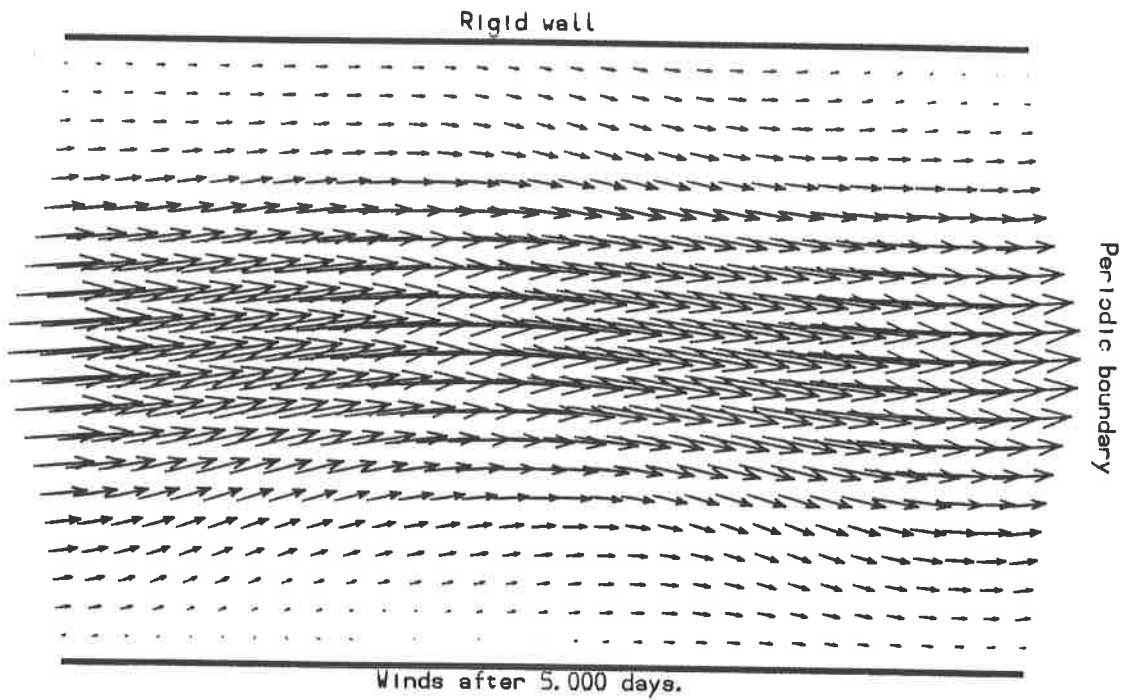


Figure 7

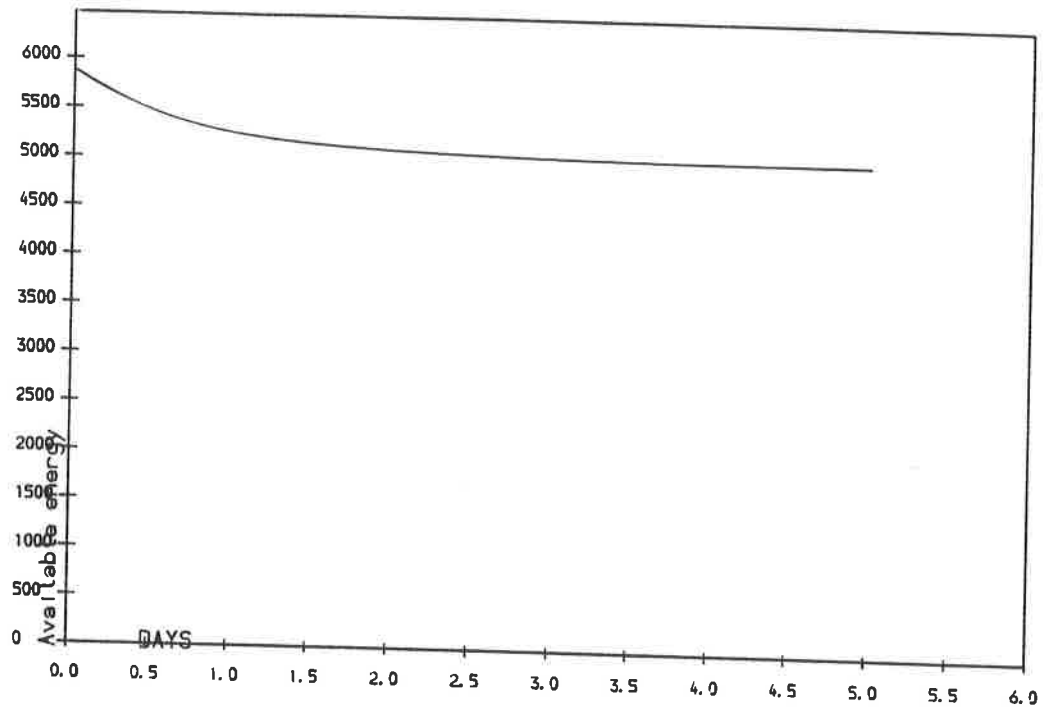


Figure 8

GRAMMELTVEDT'S PROBLEM

Solution, calculated by the Superbee scheme using
 3600 time-steps with $\Delta t = 120.00$ and $\Delta x = 200$ km.
 Initial conditions 1 were used.

The maximum height is 2225.4 metres at $\frac{1}{2}$ and the minimum height is 1767.2 metres at $\frac{1}{2}$.

Contour Key

1	→	1800.0
2	→	1850.0
3	→	1900.0
4	→	1950.0
5	→	2000.0
6	→	2050.0
7	→	2100.0
8	→	2150.0
9	→	2200.0

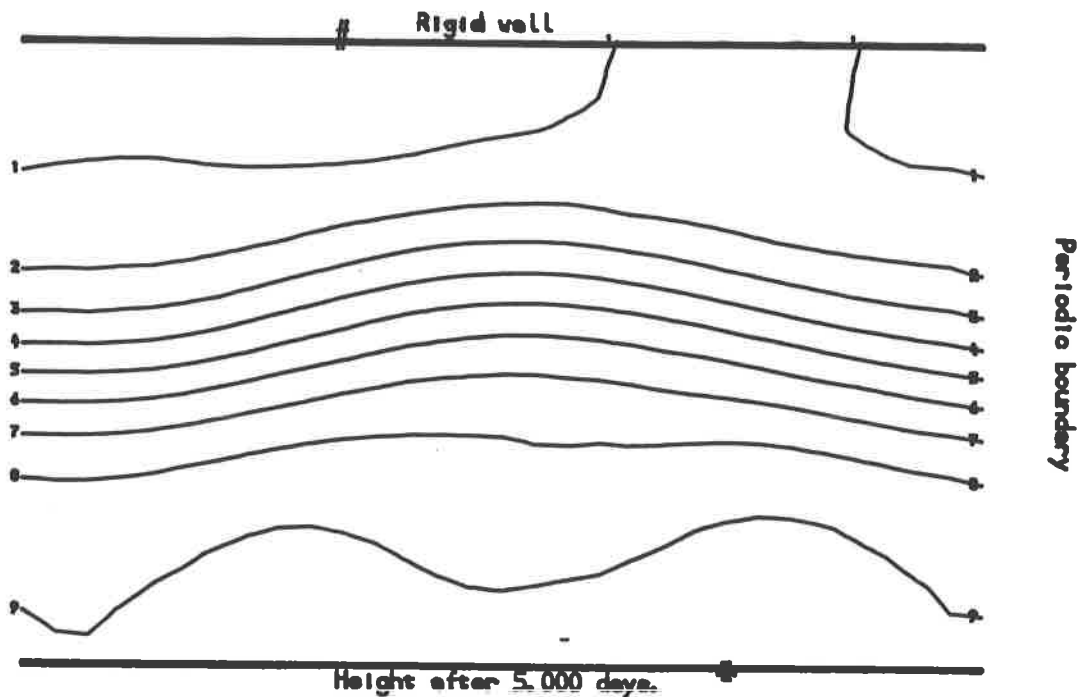


Figure 9

GRAMMELTVEDT'S PROBLEM

Solution, calculated by the Superbee scheme using
3600 time-steps with $\Delta t = 120.00$ and $\Delta x = 200$ km.
Initial conditions 1 were used.

The maximum wind speed is 26.414 metres per second.
(59.09 m.p.h.)

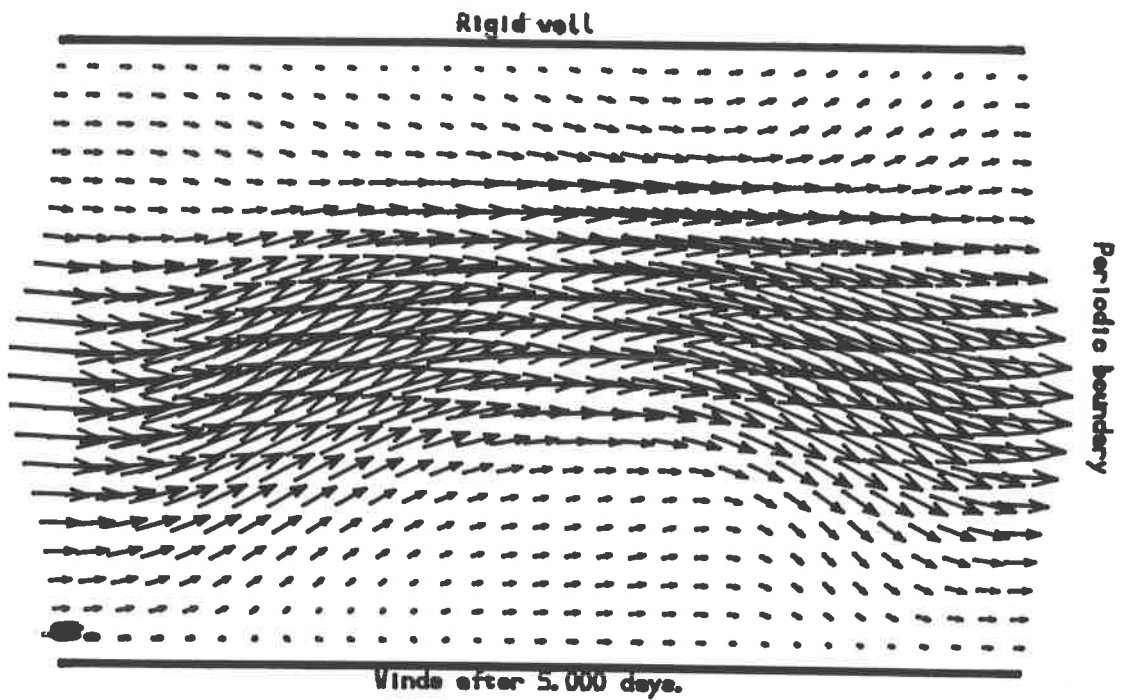


Figure 10

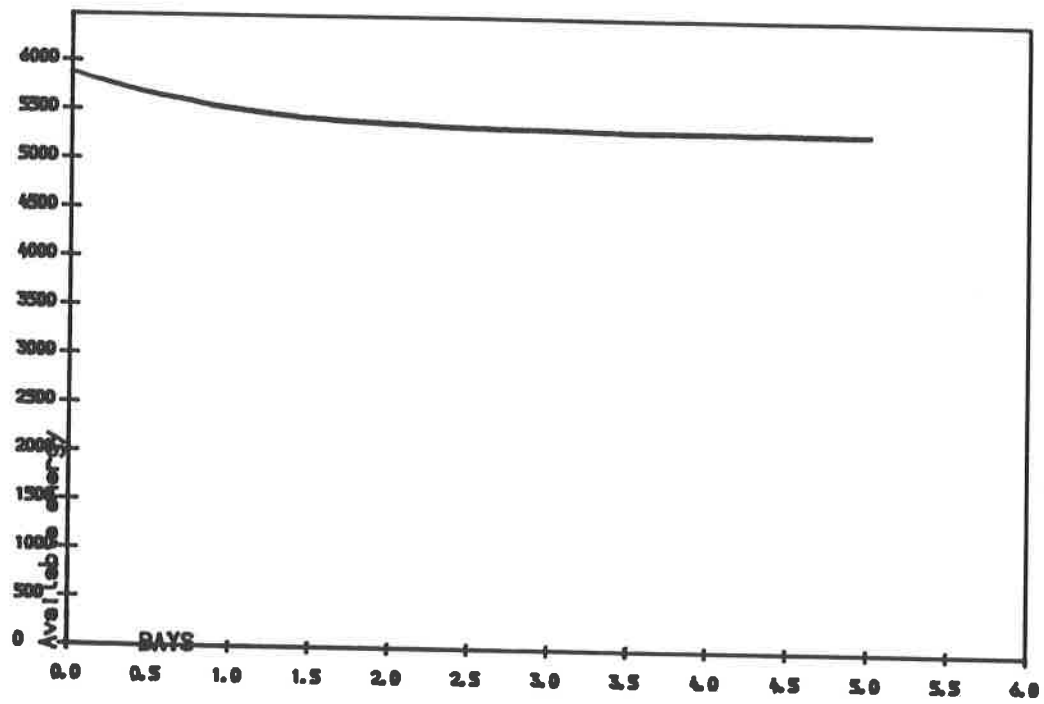
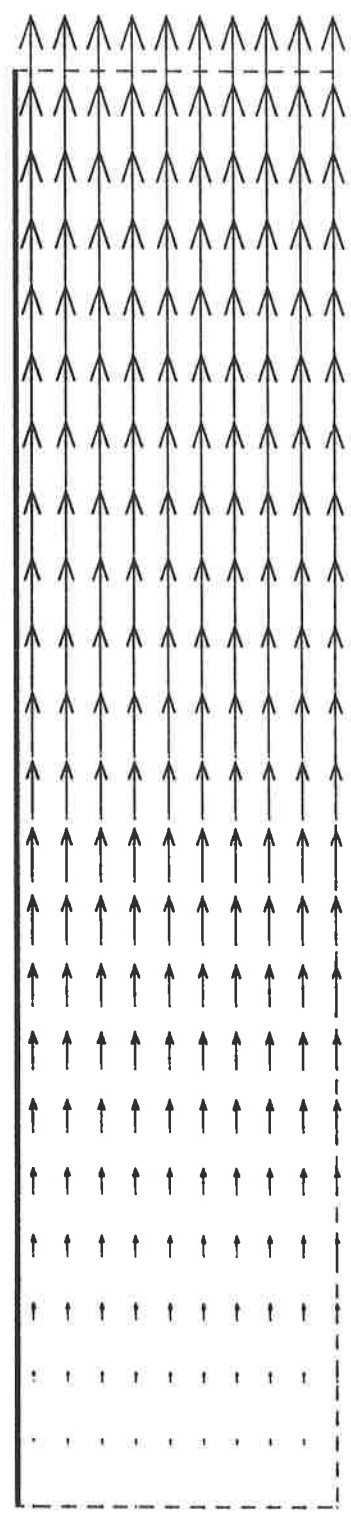
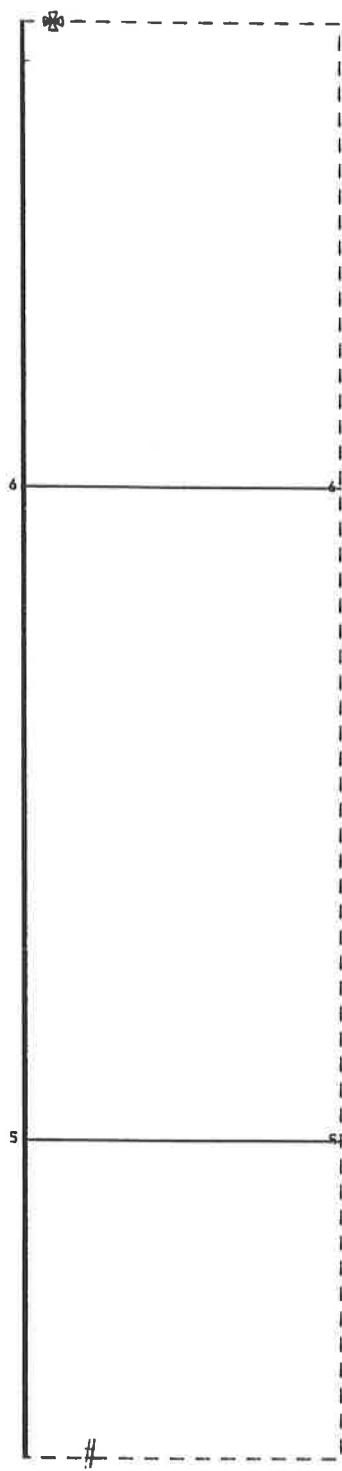


Figure 11

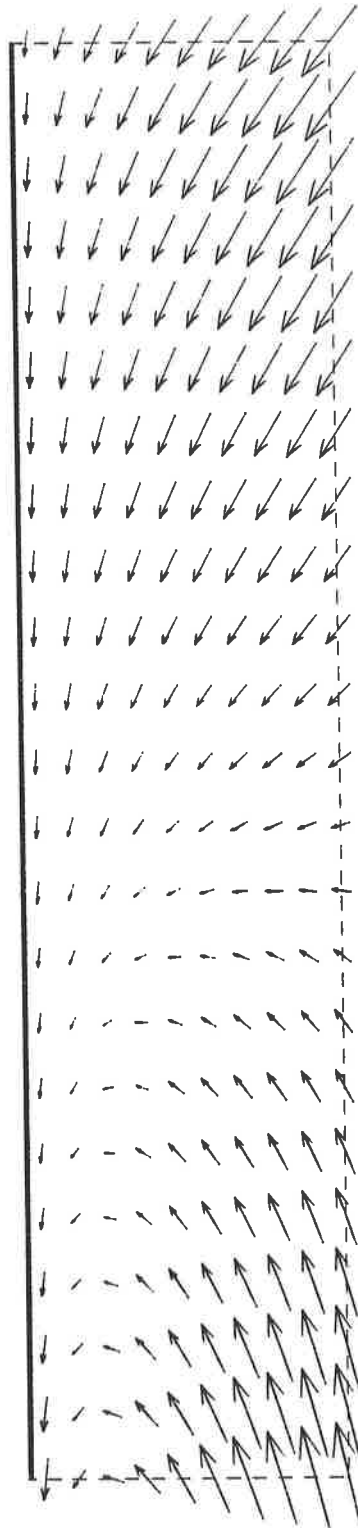
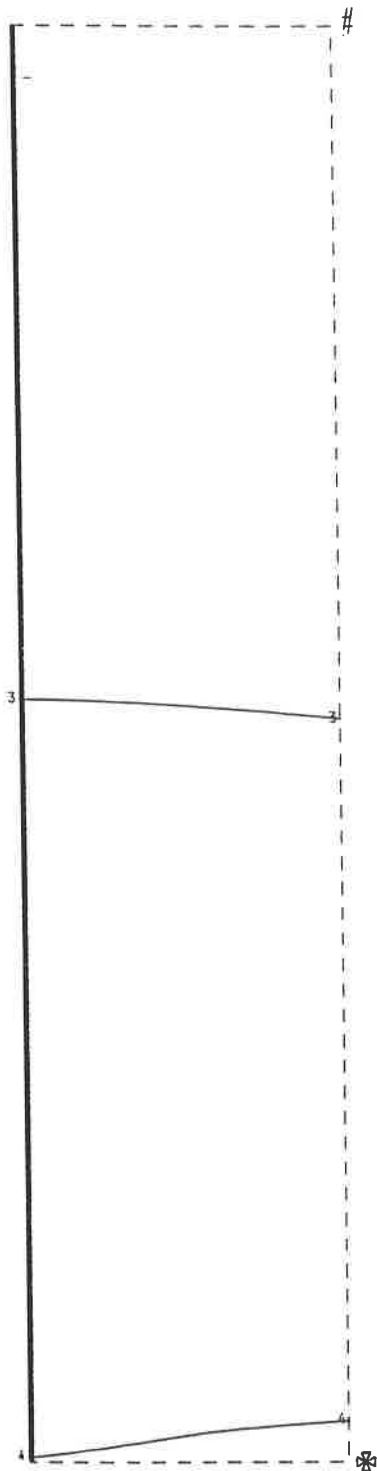


First order scheme. $\Delta t = 0.00$.
 0 time-steps used.
 Final time is 0.000 days.
 Δx is 1.05 kms.. Δy is 2.27 kms..
 The maximum height is 0.5 metres at *.
 The minimum height is 0.0 metres at #.
 The maximum velocity is 0.337
 metres per second.
 (0.75 m.p.h.)
 Tidal period is 12.42 hours.
 Tidal amplitude is 1.0 metres.
 At outflow elevation prescribed.
 At inflow elevation and tangential
 velocity prescribed.

Contour Key

1	→	-0.8
2	→	-0.6
3	→	-0.3
4	→	-0.1
5	→	0.1
6	→	0.3
7	→	0.6
8	→	0.8
9	→	1.0

Figure 12

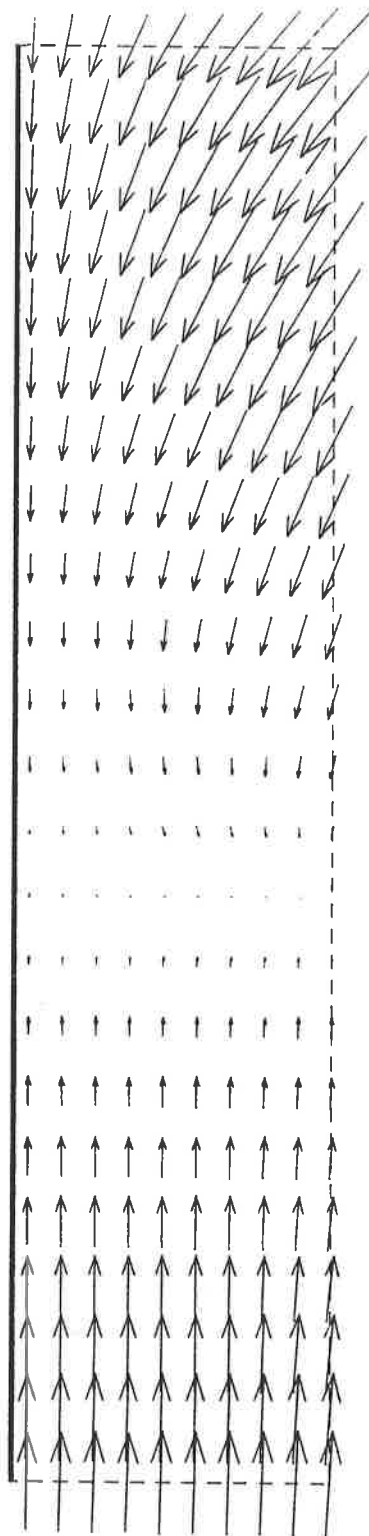
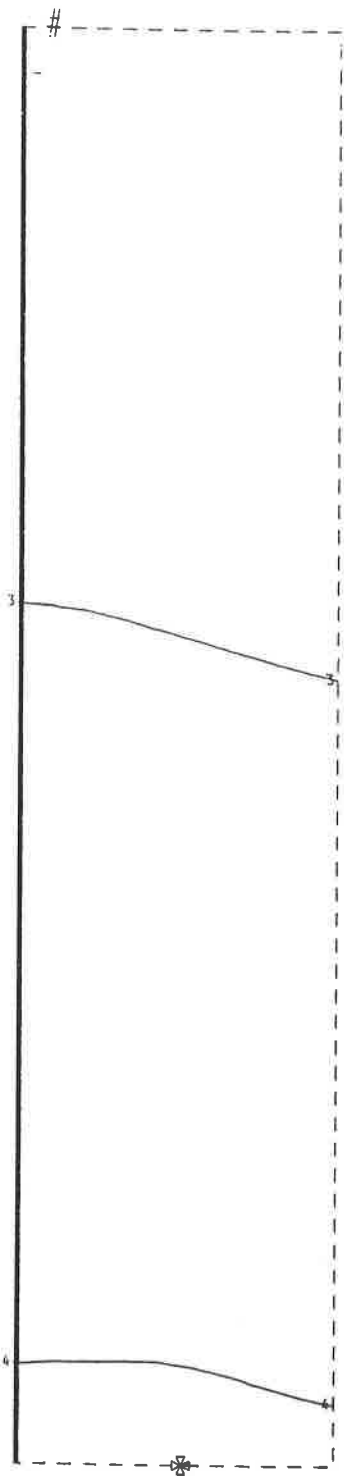


First order scheme. $\Delta t = 30.00$.
 720 time-steps used.
 Final time is 0.250 days.
 Δx is 1.05 kms.. Δy is 2.27 kms..
 The maximum height is -0.1 metres at *.
 The minimum height is -0.5 metres at #.
 The maximum velocity is 0.146 metres per second.
 (0.33 m.p.h..)
 Tidal period is 12.42 hours.
 Tidal amplitude is 1.0 metres.
 At outflow elevation prescribed.
 At inflow elevation and tangential velocity prescribed.
 Maximum CFL no. at output is 0.410.

Contour Key

1	→	-0.8
2	→	-0.6
3	→	-0.3
4	→	-0.1
5	→	0.1
6	→	0.3
7	→	0.6
8	→	0.8
9	→	1.0

Figure 13



Superbee limiter used. $\Delta t = 10.00$.
 2160 time-steps used.
 Final time is 0.250 days.
 Δx is 1.05 kms., Δy is 2.27 kms.,
 The maximum height is -0.1 metres at *.
 The minimum height is -0.5 metres at #.
 The maximum velocity is 0.122
 metres per second.
 (0.27 m.p.h.)
 Tidal period is 12.42 hours.
 Tidal amplitude is 1.0 metres.
 At outflow elevation prescribed.
 At inflow elevation and tangential
 velocity prescribed.
 Maximum CFL no. at output is 0.161.

Contour Key

- 1 → -0.8
- 2 → -0.6
- 3 → -0.3
- 4 → -0.1
- 5 → 0.1
- 6 → 0.3
- 7 → 0.6
- 8 → 0.8
- 9 → 1.0

Figure 14